



ORIGINAL ARTICLE OPEN ACCESS

The Benefits of Hierarchical Ecosystem Models: Demonstration Using EcoState, a New State-Space Mass-Balance Model

James T. Thorson¹  | Kasper Kristensen² | Kerim Y. Aydin¹ | Sarah K. Gaichas³ | David G. Kimmel⁴ | Elizabeth A. McHuron^{5,6} | Jens M. Nielsen^{4,5} | Howard Townsend⁷ | George A. Whitehouse^{1,5} 

¹Resource Ecology and Fisheries Management, Alaska Fisheries Science Center, National Marine Fisheries Service, NOAA, Seattle, Washington, USA | ²Technical University of Denmark, Lyngby, Denmark | ³Ecosystem Dynamics and Assessment Branch, Northeast Fisheries Science Center, National Marine Fisheries Service, NOAA, Woods Hole, Massachusetts, USA | ⁴Resource Assessment and Conservation Engineering, Alaska Fisheries Science Center, National Marine Fisheries Service, NOAA, Seattle, Washington, USA | ⁵Cooperative Institute for Climate, Ocean, and Ecosystem Studies, University of Washington, Seattle, Washington, USA | ⁶Marine Mammal Laboratory, Alaska Fisheries Science Center, National Marine Fisheries Service, NOAA, Seattle, WA, USA | ⁷Marine Ecosystems Division, Office of Science and Technology, National Marine Fisheries Service, Silver Spring, Maryland, USA

Correspondence: James T. Thorson (james.thorson@noaa.gov)

Received: 29 July 2024 | **Revised:** 30 October 2024 | **Accepted:** 15 November 2024

Funding: This study was supported by Cooperative Institute for Climate, Ocean, and Ecosystem Studies, University of Washington.

Keywords: Alaska pollock | eastern Bering Sea | Ecopath with Ecosim | mass-balance model | process errors | state-space model

ABSTRACT

Ecosystem models predict changes in productivity and status for multiple species, and are important for incorporating climate-linked dynamics in ecosystem-based fisheries management. However, fishery regulations are primarily informed by single-species stock assessment models, which estimate unexplained variation in dynamics (e.g., recruitment, survival, fishery selectivity, etc) using random effects. We review the general benefits of estimating random effects in ecosystem models: (1) better representing biomass cycles and trends for focal species; (2) conditioning interactions upon observed biomass for predators and prey; (3) easier replication of model results using formal estimation rather than informal model “tuning;” and (4) attributing process errors via comparison amongst different models. We then demonstrate these by introducing a new state-space model EcoState (and associated R-package) that extends mass balance dynamics from Ecopath with Ecosim. This model estimates mass balance (Ecopath) and time-dynamics (Ecosim) parameters directly via their fit to time-series data (biomass indices and fisheries catches) while also estimating the magnitude of process errors using RTMB. A real-world application involving Alaska pollock (*Gadus chalcogrammus*) in the eastern Bering Sea suggests that fluctuations in krill consumption are associated with cycles of increased and decreased pollock production. A self-test simulation experiment confirms that estimating process errors can improve estimates of productivity (growth and mortality) rates. Overall, we show that state-space mass-balance models can be fitted to time-series data (similar to surplus-production stock assessment models), and can attribute time-varying productivity to both bottom-up and top-down drivers including the contribution of individual predator and prey interactions.

This is an open access article under the terms of the [Creative Commons Attribution-NonCommercial](https://creativecommons.org/licenses/by-nc/4.0/) License, which permits use, distribution and reproduction in any medium, provided the original work is properly cited and is not used for commercial purposes.

© 2024 The Author(s). *Fish and Fisheries* published by John Wiley & Sons Ltd. This article has been contributed to by U.S. Government employees and their work is in the public domain in the USA.

1 | Introduction

Throughout ecology and fisheries, there is broad agreement that model predictions often differ from real-world observations and growing recognition that this discrepancy can be decomposed into measurement, process, and specification errors using hierarchical (a.k.a., mixed-effect or state-space) models. For example, hierarchical models are widely used in experimental analysis to account for pseudo-replication, comparative and life-history analysis to account for evolutionary similarity in model residuals (Felsenstein 1985), and population dynamics to account for unmodeled variation in demographic rates (de Valpine 2002). Hierarchical models for dynamics over time (“state-space models”) specify a simplified model for system dynamics that typically involves one or more unknown parameter (“fixed effects”) and also estimate process errors that represent how dynamics differ from this parametric model. Process errors (“random effects”) are then shrunk towards a shared mean, where the variance of these process errors can be estimated as a parameter and controls the magnitude of shrinkage (Thorson and Minto 2015).

Despite broad recognition about the importance of hierarchical modelling, they see surprisingly little use in marine ecosystem analysis. Ecosystem-based fisheries management (EBFM) has been adopted as a policy goal for ocean management agencies worldwide (FAO 2003; European Commission 2013; NOAA 2016), and ecosystem models are an essential tool for evaluating tradeoffs amongst alternative management scenarios within EBFM. Ecosystem models generally aim to represent changes in productivity and biomass for ecosystem components via trophic, technical, or other interactions (Hollowed et al. 2000). There are many types of ecosystem models with widely used software, including (to name a few) Atlantis (Fulton et al. 2011), Ecopath with Ecosim (EwE), Mizer (Scott, Blanchard, and Andersen 2014), Gadget (Begley and Howell 2004), and custom-built MICE models (Plagányi et al. 2014). Each model (and associated software) typically has different tools to “tune” parameters to improve fit to available data. For example, EwE involves a two-stage approach, where mass balance is first achieved using Ecopath and then nonequilibrium dynamics are then projected over time using Ecosim. Ecosim vulnerability parameters are sometimes tuned via fit to predator–prey-time-series (Scott et al. 2016; Bentley et al. 2024). However, time-series predictions of biomass are only calculated when tuning Ecosim (not when balancing the model in Ecopath), so this two-stage approach precludes using time-series data to tune the mass-balance parameters in Ecopath. Similarly, both Mizer and Gadget can estimate parameters representing ecosystem dynamics (Begley and Howell 2004; Spence, Blackwell, and Blanchard 2016). Although Mizer was later extended to estimate process errors (Spence et al. 2021), this has not been done for other major classes of ecosystem models.

In contrast to the dearth of hierarchical modelling for marine ecosystems, there is ongoing research to estimate time-varying parameters within single-species stock assessments using mixed-effect models (de Valpine 2002; Nielsen and Berg 2014). Stock assessments increasingly use state-space modelling (Stock and Miller 2021), and it is viewed as an

essential feature for future assessment model development (Punt et al. 2020). This increased use arises in part because state-space models can mitigate the bias that otherwise results from treating some time-varying process as if it were stationary in time (Xu, Thorson, and Methot 2020; Stock et al. 2021). Importantly, random effects can also be used to represent systematic deviations away from the parametric model, and therefore represent “mis-specification error”. In some cases, the magnitude of “mis-specification error” can be identified by estimating a new functional form for a modelled process treating a Gaussian process as random effect (Thorson, Ono, and Munch 2014), while in other cases the “process error” represents nonstationarity over time in some model parameter. In either case, estimating random effects allows an analyst to then expand the model and quantify how much the variance of process errors is reduced by a given model development. In this interpretation, process errors allow analysts to attribute unmodeled variation to specific hypothesised drivers.

We propose that hierarchical models will provide several benefits for ecosystem models and deserve adoption across the full range of ecosystem–model software. These benefits include:

1. Better representing biomass cycles and trends for focal species, i.e., where population dynamics for individual species may be driven by physical variables or interactions that are not easy to represent explicitly but whose effect is evident in available time-series. Hierarchical models can then represent these patterns as latent variables, and thereby capture apparent patterns in stock status. This model behaviour is similar to the treatment of recruitment-deviations in stock assessment, and it would allow ecosystem models to be used to measure stock status and trends.
2. Conditioning interactions upon observed biomass for predators and prey, i.e., where trends or cycles in biomass for dominant predator or forage species (which might not be represented without process errors) can then be propagated through ecosystem interactions. Hierarchical models would therefore ensure that predator consumption or forage availability matches observed patterns and that resulting predictions of species interactions are then accurately represented for other modelled taxa.
3. Easier replication of model results using formal estimation rather than informal model tuning, i.e., where models can be fitted using a statistical optimizer rather than using “forcing functions” or ad hoc model changes. By using a statistical optimizer, hierarchical models then guarantee that any analyst will arrive at the same model for a given set of data and model assumptions. This then allows the model to be updated over time by new analysts, or replicated independently during peer review.
4. Attributing observed patterns to alternative mechanistic drivers, i.e., where the analyst then seeks to identify changes in model structure that can reduce the magnitude of estimated process errors. These changes might include (A) attributing patterns to hypothesised oceanographic or ecological mechanisms that are measured as covariates, and/or (B) adding new mechanisms and functional groups to the

model. Hierarchical modelling helps by allowing models to be rapidly refitted using statistical optimisation and also allows statistical comparison amongst alternative models.

These benefits are generally observed in the relatively few ecosystem models that include process errors (Spence et al. 2021), but have not been explored for the wide range of ecosystem models.

To demonstrate these benefits, we introduce a new state-space mass-balance model that incorporates both top-down and bottom-up interactions. Using a case study representing the eastern Bering Sea centered on prey, competitors, and predators for Alaska pollock (*Gadus chalcogrammus*), we demonstrate that estimating process errors improves ecological inference and expected statistical performance. Specifically, biomass cycles for krill are associated with cycles of higher or lower productivity (and resulting biomass) for pollock, and these apparent decadal cycles are not captured without estimating process errors. We also use a simulation experiment to confirm that estimating process errors results in more accurate and precise estimates of growth and mortality rates than ignoring process errors, and that known parameter values can be recovered with reasonable precision. Finally, we conclude by discussing how hierarchical ecosystem models might mitigate capacity constraints that hamper wider adoption and tactical application of ecosystem models.

2 | Methods

We demonstrate the general utility of hierarchical modelling for ecosystem analysis by introducing an extension of Ecopath with Ecosim that estimates both parametric uncertainty and the variance of residual variation in biomass dynamics (“process errors”). The associated R-package *ecostate* uses RTMB (Kristensen 2024a) to implement automatic differentiation and fit process errors via maximum marginal likelihood. Our demonstration is intended in part to demonstrate that automatic differentiation and the Laplace approximation (via RTMB) can be used to fit nonlinear ordinary differential equations with many variables, as required for many ecosystem models. Parametric uncertainty and process errors have been added previously to other ecosystem models, e.g., Mizer (Spence, Blackwell, and Blanchard 2016; Spence et al. 2021), but EwE has typically separated mass balance (Ecopath) from biomass projections (Ecosim) and therefore precluded estimating mass-balance parameters using time-series data. *Ecostate* is therefore the first (to our knowledge) model to formally estimate mass-balance and process-error parameters using mass-balance dynamics, and mass balance provides an avenue to incorporate bottom-up dynamics (i.e., where prey availability affects predator productivity).

2.1 | Benefits of Hierarchical Modelling for Mass-Balance Ecosystem Models

EcoState demonstrates the advantages of hierarchical ecosystem modelling relative to previous mass-balance models (Christensen and Walters 2004; Lucey, Gaichas, and Aydin 2020) in several ways:

1. *Joint modelling*: It combines the mass balance done by Ecopath with the dynamical projection from Ecosim within a single statistical model. It therefore replaces a two-stage workflow with a single model, and allows the model to be easily refitted (including rebalancing the population scale) when adding/dropping taxa or data. This involves estimating equilibrium population biomass, nonequilibrium initial conditions, catchability coefficients, the variance of process errors via fit to available time-series, as well as predator–prey vulnerability, production, and consumption per biomass. Ecosim has previously been fitted to estimate vulnerability parameters using likelihood or sum-of-squares methods (Gaichas et al. 2012; Scott et al. 2016; Bentley et al. 2024), but we do not know of efforts to jointly estimate mass-balance (Ecopath) and vulnerability (Ecosim) parameters.
2. *Process errors*: By estimating process errors, we ensure that estimated mass $\beta_{s,t}$ is shrunk towards measured values $q_s b_{s,t}$ whenever measurements are available. This then ensures that modelled consumption is shrunk towards the quantity expected given that measured mass, i.e., that systematically over- or underestimating mass for a variable relative to observations does not propagate into over- or under-estimated consumption for interacting species. For variables that have no biomass measurements, dynamics are then inferred based on time-varying productivity resulting from changes in modelled consumption (and resulting gain and loss rates) conditional upon those estimated process errors.
3. *Model bridging*: If the analyst chooses to specify all parameters and turn off process errors, then dynamics will be similar to those from Ecopath and Ecosim. This then facilitates model building, i.e., by starting with published EwE models and progressively “turning on” different parameters and/or process errors.
4. *Forecast variance*: If the analyst chooses to model future years with no available data regarding absolute or relative mass, they must still specify a value for catch in those future years. Having done this, the model will automatically propagate uncertainty about process errors $\epsilon(t)$ and resulting uncertainty about biomass $\beta(t)$ in those future years.
5. *Exploring ecosystem modules*: Finally, the analyst may want to isolate interactions amongst a small subset of taxa (“species module;” Holt 1997). The model still estimates consumption amongst those taxa that are retained but typically identifies decreased ecotrophic efficiency for those taxa whose predators are excluded. This addresses ongoing calls for “minimal realistic models,” whether using mass-balance dynamics (Walters, Christensen, and Pauly 1997) or otherwise (Plagányi et al. 2014).

These features are common in modern stock assessment models, but novel for mass-balance ecosystem models.

2.2 | Mass-Balance Based on Ecopath

EcoState is a mass-balance model that can be solved for equilibrium mass of different ecosystem components (e.g., detritus,

primary producers, consumers, and predators) that are coupled via consumption, production, and detrital production/decomposition rates (Polovina 1984). EcoState tracks mass-vector $\boldsymbol{\beta}$ composed of mass β_s for each functional group or detrital pool (called “variables” in the following), indexed by $s \in \{1, 2, \dots, S\}$ where S is the total number of variables. Each variable is then specified as an (1) autotroph (i.e., primary producer), (2) heterotroph (i.e., consumer or predator), or (3) detritus. We attempt to use mathematical notation following guidelines from Edwards and Auger-Méthé (2019), particularly by using Greek letters for state variables (e.g., biomass), Roman for parameters and data, vector-matrix notation (i.e., lowercase italic for scalars), and avoiding the use of multiple letters for a single parameter. This results in some departures from previous Ecopath and Ecosim notation (see Table S1 for a summary of all notation), although we use similar symbols where practical. We refer to the combination of autotrophs and heterotrophs as “biomass” or “taxa,” and we also index variables as prey $i \in \{1, 2, \dots, S\}$ and predator $j \in \{1, 2, \dots, S\}$ in expressions where prey and predators are both included. Each variable s at equilibrium is assumed to have a fixed ratio of production to biomass p_s , consumption to biomass w_s (where $w_s = \text{NA}$ for detritus and primary producers), and a fixed $S \times S$ diet matrix \mathbf{D} containing the proportion $d_{i,j}$ of diet provided by each potential prey i for predator j (where $d_{i,j} = 0$ for detritus and primary producers as “predators” j and all “prey” i). Finally, each variable is assumed to have mass that is “used” in the system (i.e., consumed by predators or removed by fisheries), and this is represented as ecotrophic efficiency e_s .

Similar to Ecopath, equilibrium in EcoState occurs for each variable when its gain matches loss rate. To match notation that is common in stock-assessment models, we define equilibrium mass $\bar{\beta}_s$ as the average mass in the absence of fishing:

$$\underbrace{\bar{\beta}_i}_{\text{Equilibrium biomass for prey } i} \times \underbrace{p_i}_{\text{Prey production per biomass}} \times \underbrace{e_i}_{\text{Prey ecotrophic efficiency}} = \sum_{j=1}^S \left(\underbrace{d_{i,j}}_{\text{Proportion of diet for predator } j \text{ by prey } i} \times \underbrace{\bar{\beta}_j}_{\text{Equilibrium biomass for predator } j} \times \underbrace{w_j}_{\text{Predator consumption per biomass}} \right) \quad (1)$$

Later, we incorporate fishing mortality to project ecosystem dynamics away from this unfished equilibrium. Unknown values in Equation (1) can be solved by re-expressing it in vector-matrix notation. Specifically, gains (left side of Equation 1) are written as $\boldsymbol{\beta} \odot \mathbf{p} \odot \mathbf{e}$, where e.g. $\boldsymbol{\beta} \odot \mathbf{p}$ is the Hadamard (elementwise) product of two vectors $\boldsymbol{\beta}$ and \mathbf{p} . Similarly, losses (right side of Equation 1) are $\mathbf{D}(\boldsymbol{\beta} \odot \mathbf{w})$. Equilibrium biomass $\bar{\boldsymbol{\beta}}$ is achieved when these rates match, i.e. $\bar{\boldsymbol{\beta}} \odot \mathbf{p} \odot \mathbf{e} = \mathbf{D}(\bar{\boldsymbol{\beta}} \odot \mathbf{w})$, which can be solved for some combination of equilibrium biomass $\bar{\boldsymbol{\beta}}$ and ecotrophic efficiency (Appendix S2). Given this equilibrium, we then calculate equilibrium consumption $\bar{\mathbf{C}}$:

$$\bar{\mathbf{C}} = \mathbf{D} \odot (\mathbf{1}(\bar{\boldsymbol{\beta}} \odot \mathbf{w})^T) \quad (2)$$

where $\mathbf{1}$ is a column-vector of 1s such that $\mathbf{1}(\bar{\boldsymbol{\beta}} \odot \mathbf{w})^T$ is a matrix of equilibrium consumption $\boldsymbol{\beta} \odot \mathbf{w}$ for each predator, repeated as separate rows for each prey.

The fitted model can then be used to solve for equilibrium levels of a specified tracer y_s for each taxon s . This tracer \mathbf{y} represents any physical or theoretical quantity that is tracked as it progresses through the food chain via consumption under the expression $\mathbf{z} = \mathbf{z}\mathbf{C}^* + \mathbf{y}$ where \mathbf{C}^* is the consumption $c_{i,j}$ for each prey i by each predator j rescaled to sum to one for each predator to represent a proportion, and \mathbf{z} is the equilibrium concentration of a tracer to be estimated. For example, trophic level is defined as a tracer such that $\mathbf{z} = \mathbf{z}\mathbf{C}^* + \mathbf{y}$, where $\mathbf{y} = \mathbf{1}$ is the increase in trophic level each time mass is consumed. This simultaneous equation for trophic level is then solved as $\mathbf{z} = \mathbf{1}^T(\mathbf{I} - \mathbf{C}^*)^+$, where $(\mathbf{I} - \mathbf{C}^*)^+$ is the Penrose-Moore pseudoinverse of $\mathbf{I} - \mathbf{C}^*$ and $\mathbf{1}^t$ is a row-vector of 1s. Alternatively, we define tracer \mathbf{y} , e.g., as an indicator vector that is 1 for the base of the pelagic food chain and 0 otherwise, and then calculate the proportion of biomass for each taxon that results from pelagic production as $\mathbf{z} = \mathbf{y}^T(\mathbf{I} - \mathbf{C}^*)^+$.

2.3 | Time-Dynamics Based on Ecosim

After Ecopath is applied to achieve mass balance for all species, Ecosim is separately used to simulate dynamics forward in time (Pauly, Christensen, and Walters 2000; Christensen and Walters 2004). By contrast, EcoState uses proposed parameters to solve for missing values that achieve mass balance, and simultaneously uses those parameters to project dynamics for all variables at times $t \in \{t_1, t_2, \dots, T\}$ while integrating dynamics

over the interval between these times (e.g., from t_1 to t_2). We discretize time into years in the following, but future research could incorporate seasonal (e.g., monthly) variation using a higher-resolution time-interval with no change in equations or code. Similarly, future research could explore how fishing mortality affects the prey production p_i and predator consumption w_i via its impact on age-structure (Aydin 2004), although we do not do so here.

Adapting notation from Lucey, Gaichas, and Aydin (2020), EcoState represents similar dynamics as Ecosim by specifying a differential equation for mass:

$$\frac{d}{dt}\boldsymbol{\beta}(t) = \begin{pmatrix} \underbrace{\mathbf{g}(t)}_{\text{Growth rate}} - \underbrace{\mathbf{m}(t)}_{\text{Natural mortality rate}} - \underbrace{\mathbf{f}(t)}_{\text{Fishing mortality rate}} \end{pmatrix} \odot \boldsymbol{\beta}_t \quad (3)$$

where $f_s(t)$ is fishing mortality rate and both growth rate $g_s(t)$ and loss rate $m_s(t)$ are calculated from annual consumption rate $\mathbf{C}(t)$, representing the mass $c_{i,j}(t)$ of prey i consumed by predator j , where $\frac{d}{dt}\boldsymbol{\beta}(t) = \mathbf{0}$ whenever $\boldsymbol{\beta}_t = \bar{\boldsymbol{\beta}}$ in the absence of fishing. Future studies could include net migration, although this is often not considered in stock-assessment models and therefore ignored here as well. This equation also assumes that parameters in growth and natural mortality rates are stationary over time. Future studies could address ontogenic shifts in diet by incorporating stanzas (i.e., age-structured models for selected taxa) and could estimate time-varying diet or other parameters by fitting directly to diet time-series data. EcoState provides a general platform for these extensions, although we do not implement them here.

Consumption rate $\mathbf{C}(t)$ varies around equilibrium consumption $\bar{c}_{i,j}$ based on predator and prey mass:

$$c_{i,j}(t) = \underbrace{\bar{c}_{i,j}}_{\text{equilibrium consumption rate}} \times \underbrace{\frac{x_{i,j} \frac{\beta_j(t)}{\beta_j}}{x_{i,j} - 1 + \frac{\beta_j(t)}{\beta_j}}}_{\text{predator functional response}} \times \underbrace{\frac{\beta_i(t)}{\beta_i}}_{\text{prey functional response}} \quad (4)$$

where \mathbf{X} is the matrix of predator-prey vulnerability parameters containing the vulnerability $x_{i,j}$ for prey i to predator j (Aydin 2004 equation 1; Plagányi and Butterworth 2004). Our model for consumption (Equation 4) does not include those processes that are eliminated using default values in EwE as implemented in the Rpath package (Lucey, Gaichas, and Aydin 2020), and see Appendix S1 for more discussion. Given that diet $d_{i,j} = 0$ for each column j associated with autotrophs or detritus, consumption $\bar{c}_{i,j} = 0$ and $c_{i,j}(t) = 0$ for autotrophs and detritus as well.

Loss rates $m_s(t)$ are calculated separately for detritus and biomass variables. Specifically, loss for biomass variables (autotrophs and heterotrophs) results from consumption and unmodeled natural mortality, while loss for detritus results from consumption and a constant export rate:

$$m_s(t) = \underbrace{\frac{\sum_{j=1}^S c_{s,j}(t)}{\beta_s(t)}}_{\text{Predation rate}} + \begin{cases} \underbrace{p_s(1-e_s)}_{\text{Residual natural mortality rate}} & \text{if } s \text{ is autotroph or heterotroph} \\ \underbrace{v_s}_{\text{Export rate}} & \text{if } s \text{ is detritus} \end{cases} \quad (5)$$

where residual natural mortality $p_s(1-e_s)$ accounts for predation by unmodeled taxa, senescence, and disease. As a taxon s has more predators explicitly modelled, ecotrophic efficiency $e_s \rightarrow 1$ such that residual mortality $p_s(1-e_s) \rightarrow 0$, while a taxon with no modelled predators ($e_s = 0$) will have residual natural mortality of p_s . This one-to-one relationship between residual mortality and ecotrophic efficiency (for a given production-per-biomass) is necessary to achieve mass balance, such that the proportion of consumptive vs. residual natural mortality for each taxon is determined by how many of its predators are represented. Similarly, v_s is detritus export (e.g., decomposition or turnover) rate, which is defined to ensure that net detritus accumulation matches net consumption plus export at equilibrium:

$$\bar{v}_s v_s = \underbrace{\sum_{i=1}^S \sum_{j=1}^S u_j \bar{c}_{i,j}(t)}_{\text{Detritus accumulation}} + \sum_{j=1}^S \bar{\beta}_j p_j (1-e_j) - \underbrace{\sum_{j=1}^S \bar{c}_{s,j}(t)}_{\text{Detritus consumption}} \quad (6)$$

where u_j is the proportion of consumption that is not assimilated for predator j (with $u_j = 0.2$ by default) such that total unassimilated consumption $\sum_{i=1}^S \sum_{j=1}^S u_j c_{i,j}(t)$ then accumulates as detritus. Similarly, $\sum_{j=1}^S \bar{\beta}_j p_j (1-e_j)$ is the total residual natural mortality, which we assume flows to detritus following Walters, Christensen, and Pauly (1997).

Gain rate $g_s(t)$ is then calculated differently for producers, consumers, and detritus:

$$g_s(t) = \begin{cases} \frac{p_s}{w_s} \times \frac{\sum_{i=1}^S c_{i,s}(t)}{\beta_s(t)} & \text{if } s \text{ is heterotroph} \\ \frac{p_s \bar{\beta}_s}{\beta_s(t)} \times \frac{x_{s,s} \frac{\beta_s(t)}{\beta_s}}{x_{s,s} - 1 + \frac{\beta_s(t)}{\beta_s}} & \text{if } s \text{ is autotroph} \\ \frac{\sum_{i=1}^S \sum_{j=1}^S u_j c_{i,j}(t) + \sum_{j=1}^S \beta_j(t) p_j (1-e_j)}{\beta_s(t)} & \text{if } s \text{ is detritus} \end{cases} \quad (7)$$

where the gain rate for heterotrophs is calculated as total consumption across all prey divided by predator biomass, and multiplied by the ratio of production-per-biomass and consumption per biomass (termed growth efficiency). Alternatively, autotrophs do not consume other modelled taxa, so their density-dependence is modelled via a Michaelis-Menten (a.k.a. half-saturation) function (Walters, Christensen, and Pauly 1997 equation 5; Gaichas et al. 2012 equation 6) where $p_s \bar{\beta}_s$ is their equilibrium production and $\frac{x_{s,s} \frac{\beta_s(t)}{\beta_s}}{x_{s,s} - 1 + \frac{\beta_s(t)}{\beta_s}}$ has

the same form as the predator functional response for heterotrophs (Equation 4). Finally, detritus accumulates from the unassimilated consumption for all predators and prey $\sum_{i=1}^S \sum_{j=1}^S u_j c_{i,j}(t)$, as well as unmodeled mortality rate $\sum_{j=1}^S \beta_j(t) p_j (1-e_j)$ for each taxon as prey (Walters, Christensen, and Pauly 1997).

Finally, EcoState estimates an instantaneous fishing mortality rate for any variable with catch data in a given year. To do

so, EcoState tracks the harvest η_s for each variable s , and treats vector $(\boldsymbol{\beta}, \boldsymbol{\eta})$ of length $2S$ as the augmented set of state variables. Harvest is itself calculated from fishing mortality rates $\boldsymbol{\phi}(t)$ composed of $\phi_k(t)$ for each fishery k , where each fishery has species selectivity $r_{s,k}$ such that the fishing mortality rate for each species is $\mathbf{f}(t) = \mathbf{R}\boldsymbol{\phi}(t)$. We also include an additional process-error term $\boldsymbol{\epsilon}(t) \odot \boldsymbol{\beta}(t)$, where $\epsilon_s(t)$ represents unmodeled variation in population growth rates for taxon s .

$$\frac{d}{dt}\boldsymbol{\beta}(t) = \left(\underbrace{\mathbf{g}(t)}_{\substack{\text{Growth} \\ \text{rate}}} - \underbrace{\mathbf{m}(t)}_{\substack{\text{Natural} \\ \text{mortality} \\ \text{rate}}} - \underbrace{\mathbf{f}(t)}_{\substack{\text{Fishing} \\ \text{mortality} \\ \text{rate}}} + \underbrace{\boldsymbol{\epsilon}(t)}_{\substack{\text{Process error} \\ \text{in biomass rate}}} \right) \odot \boldsymbol{\beta}_t + \frac{d}{dt}\boldsymbol{\eta}(t) = \mathbf{f}(t) \odot \boldsymbol{\beta}(t) \quad (8)$$

Including process errors $\epsilon_{s,t}$ in the differential equation for mass (Equation 8) implies that mass balance is maintained on average over time, but not exactly in any single year. We interpret any short-term departure from mass balance as representing processes that are not well approximated in the model, i.e., annual variation in ecotrophic efficiency, detrital export, growth efficiency, residual natural mortality, or resulting from unmodeled environmental conditions.

2.4 | Model Fitting

To fit this model, EcoState defines a set of coefficients $\boldsymbol{\theta} = (\mathbf{p}, \mathbf{w}, \mathbf{D}, \bar{\boldsymbol{\beta}}, \boldsymbol{\phi}(t), \boldsymbol{\delta}, \boldsymbol{\epsilon}(t), \mathbf{q}, \boldsymbol{\sigma}^2, \boldsymbol{\tau}^2, \boldsymbol{\nu}^2)$. These are then used to project biomass $\boldsymbol{\beta}(t)$ through time and model predictions are compared with available data to calculate a joint likelihood. We then treat process errors $\boldsymbol{\epsilon}(t)$ as random effects, and integrate across their values using the Laplace approximation to calculate the marginal likelihood, which is feasible at high precision because we are using automatic differentiation (Skaug and Fournier 2006). We optimise the log-marginal likelihood to identify the maximum likelihood estimate for selected parameters, and compute Empirical Bayes predictions of random effects by optimising the joint likelihood with respect to random effects using the MLE for fixed effects. Finally, we use a generalisation of the delta method to compute standard errors and predictive errors for fixed and random effects (Kass and Steffey 1989). EcoState is implemented in the R statistical environment (R Core Team 2023) using RTMB (Kristensen 2024a). RTMB provides a simplified interface to the Template Model Builder library (Kristensen et al. 2016), which uses automatic differentiation (AD) for efficient calculation of model derivatives, as well as the derivative of the Laplace approximation. We check model convergence by confirming that the gradient of the log-marginal likelihood with respect to each fixed effect is less than 0.001, and the matrix of 2nd derivatives of the negative log-marginal likelihood (the outer Hessian matrix) is positive definite.

In the following, we assume that the diet matrix \mathbf{D} is known and explore either fixing \mathbf{p} and \mathbf{w} or estimating \mathbf{p} and \mathbf{w} using

informative Bayesian priors. We encourage future research to adapt Bayesian diagnostics for ecosystem-modelling contexts (Monnahan 2024), but do not explore it in detail here. Similarly, the user can control what combination of other parameters are estimated or fixed at known values. In particular, the user must specify (or estimate) a value for either ecotrophic efficiency e_s or equilibrium biomass $\bar{\beta}_s$ (but not both) for each taxon, and EcoState then solves for the unspecified value (e.g., e_s if $\bar{\beta}_s$ is treated as a parameter) for each taxon (see Appendix S2). This specified value can be fixed a priori (e.g., fixing ecotrophic efficiency $e_s = 1$ for a taxon s for which all predators are modelled) or estimated as a fixed effect (e.g., estimating equilibrium biomass $\bar{\beta}_s$ for a taxon that has an absolute index of biomass to inform population scale, or fishery depletion is informative about population scale). We therefore estimate equilibrium biomass and/or ecotrophic efficiency for some set of taxa while jointly projecting biomass $\beta_s(t)$ in discretised times $t \in \{1, 2, \dots, T\}$.

We specifically assume that the biomass β_s for each variable s starts at some initial condition, $\beta_s(t_1) = \bar{\beta}_s \delta_s$, where δ_s is the ratio of initial to equilibrium mass for taxon s , where $\log(\delta_s) = 0$ by default. At the beginning of each time-interval, we similarly specify that annual harvest $\boldsymbol{\eta}(t) = \mathbf{0}$ for all taxon. We then integrate the differential equation over the interval $(t, t + 1)$ using specified values of $\mathbf{p}, \mathbf{w}, \mathbf{e}, \mathbf{D}, \bar{\boldsymbol{\beta}}, \boldsymbol{\phi}(t)$, and $\boldsymbol{\epsilon}(t)$, and record the integrated value $\boldsymbol{\eta}(t + 1)$ at the end of each interval as the predicted catch occurring for each taxon in that interval from t to $t + 1$. In the following, we specifically use a third-order Adams-Bashford-Moulton method, but also provide an alternative fourth-order Runge-Kutta method where both are adapted from the *pracma* package in R (Borchers 2023). We initially explored alternative ordinary differential equation (ODE) solvers that are provided by the *deSolve* package in R (Soetaert, Petzoldt, and Setzer 2010) using package *RTMBode* (Kristensen 2024b), but found that this approach was not sufficiently flexible to deal with the Laplace approximation given the specified structure of EcoState. We continue this integration for all $t \in \{1, 2, \dots, T\}$, while recording biomass $\boldsymbol{\beta}(t)$ and harvest $\boldsymbol{\eta}(t)$ at the end of each year. We confirmed that results are unchanged when increasing the number of sub-intervals evaluated when applying the ODE solver for Equation (8).

We then calculate the joint likelihood by specifying that biomass measurements follow a lognormal distribution:

$$\log(b_s(t)) \sim \text{Normal}(\log(q_s \beta_s(t)), \sigma_s^2) \quad (9)$$

where q_s is the catchability coefficient representing the proportion of biomass that is available to a monitoring program for taxon s , σ_s^2 is a user-specified variance for the any biomass measurements, and where $b_{s,t} = \text{NA}$ ignores this component from the likelihood. Similarly, we specify a lognormal distribution for catches:

$$\log(h_s(t)) \sim \text{Normal}(\log(\eta_s(t)), \nu_s^2) \quad (10)$$

where ν_s^2 is a user-specified variance for the any catch data, and where $h_s(t) = \text{NA}$ ignores this component from the likelihood. Finally, we specify a distribution for process errors:

$$\epsilon_s(t) \sim \text{Normal}(0, \tau_s^2) \quad (11)$$

where τ_s^2 and ϵ_s can be fixed at zero a priori to “turn off” process errors for any taxa s , or τ_s^2 can be estimated as a fixed effect and ϵ_s as a random effect.

2.5 | Case Study: Productivity and Mortality for Alaska Pollock in the Eastern Bering Sea

To illustrate the potential benefits of hierarchical ecosystem models using EcoState, we fit it to survey data and catches for 11 variables in the eastern Bering Sea from 1982 to 2021 (Table S2). This example includes major predators, prey, and competitors for Alaska pollock, including three fishes (pollock; Pacific cod, *Gadus macrocephalus*, hereafter referred to as cod; and arrowtooth flounder *Atheresthes stomias*), one autotroph (pelagic producers), one detritus variable, five intermediate consumers (copepods, krill, demersal invertebrates, benthic microbes, and other pelagic zooplankton), and one predator (northern fur seal, *Callorhinus ursinus*). We use productivity and diet parameters ($\mathbf{p}, \mathbf{w}, \mathbf{D}$, see Table S3) from previous Rpath and EwE analysis (Aydin et al. 2007; Whitehouse et al. 2021), which are aggregated using biomass-weighted averages of variables from those models. However, we use updated consumption w_s for northern fur seals to better account for energy needs while in the eastern Bering Sea. We do not use any information about ecosystem scale (ecotrophic efficiency e_s or equilibrium biomass β_s) from a previous mass-balance model to avoid “double-dipping” on data that might have informed previous models and which we also use during model fitting. We fit the model using 20 sub-intervals for the Adams-Bashforth solver per year but confirm that results are (essentially) unchanged when increasing this to 30 sub-intervals per year.

This example estimates annual fishing mortality using catch data for the three fishes (pollock, cod, and arrowtooth flounder). We assume that catches arise from three separate fisheries (i.e., the fishery selection matrix \mathbf{R} is an identity matrix), and specify measurement error $v_s = 0.1$. We also fit to biomass time-series calculated using a design-based estimator applied to survey data from an annual bottom-trawl survey in the eastern Bering Sea (Lauth and Conner 2016), and a biomass-time series for northern fur seal (from McHuron et al. 2020), and see Appendix S3 for details. Cod and arrowtooth are bottom-associated species, and we therefore assume that the biomass time-series in the eastern Bering Sea is an absolute index of biomass (i.e., catchability coefficient $q_s = 1$). Similarly, the northern fur seal biomass index is generated from population models estimating numbers at age for St. Paul and St. George Islands (we only use values from years with direct surveys occurring at those sites), and we also assume that it is an absolute index of biomass. Given this assumption, we then estimate equilibrium biomass $\bar{\beta}_s$ and initial abundance relative to equilibrium δ_s for cod, arrowtooth, and northern fur seal as fixed effects. By contrast, pollock has both demersal and pelagic components (Monnahan et al. 2021), so we treat the bottom-trawl survey as a relative abundance index and therefore estimate catchability q_s (which we expect will be < 1) and initial abundance relative to equilibrium δ_s . Similarly, we fit to a relative abundance index (i.e., estimating catchability coefficient q_s) for biomass indices for copepods and other

pelagic zooplankton (from a fall surface trawl survey), krill (from a summer acoustics survey), and pelagic primary producers (from satellite chlorophyll-*a* concentrations averaged from May to October).

For all eight variables without an absolute biomass index, we estimate population scale by specifying that ecotrophic efficiency $e_s = 1$. However, future applications could instead use Bayesian priors on ecotrophic efficiency and/or equilibrium biomass to relax the assumption that $e_s = 1$ for those eight variables. Specifying $e_s = 1$ results in all mortality being due to consumption for these functional groups (i.e., residual mortality $p_s(1 - e_s) = 0$), such that predator and prey are tightly coupled. We specify measurement error $\sigma_s = 0.1$ for all abundance indices. We also specify vulnerability $x_{i,j} = 2$ (the default from Rpath and EwE) for all heterotrophs, and $x_{i,j} = 91$ (the upper bound from Rpath) for the autotroph. Finally, we estimate annual process errors for five taxa (pollock, cod, arrowtooth, copepods, and northern fur seal) as random effects and estimate the standard deviation of process-error variation τ_s for each of these taxa as fixed effects.

We specifically compare estimates from four contrasting specifications of EcoState:

1. *Full*: Estimating process errors and fishing mortality to estimate annual consumption and productivity resulting from estimated biomass for predators and prey;
2. *Priors*: Estimating the same model as *Full*, but also estimating productivity per biomass p_s and consumption per biomass w_p for each of pollock, cod, arrowtooth, copepods, northern fur seal, and euphausiids, while specifying a lognormal likelihood penalty with a log-standard deviation of 0.1;
3. *No process errors*: Turning off process errors to estimate the consumption and productivity that would be expected without estimating annual variation in ecological dynamics;
4. *No catches or process errors*: Turning off process errors and ignoring fishing mortality (i.e., specifying $h_s(t) = 0$ for all taxa), to estimate the equilibrium conditions that are otherwise expected.

Finally, we also extract a comparable measure of combined (male and female) biomass from stock-assessment models where available, e.g., total biomass for Pacific cod using model 23.1.0.d (Barbeaux et al. 2023 New York: R package version 2.4.4, table 2.26), age 3+ biomass for Alaska pollock (Ianelli et al. 2023 table 26), and age-1+ biomass for arrowtooth flounder (Shotwell et al. 2023 table 6.13).

For each model, we record the annual growth rate $g_s(t)$ and mortality rate $m_s(t)$. We use this to illustrate how variation in predators and prey has resulted in time-varying production. We also decompose growth rate and mortality rate per biomass into the contributions from individual predators and prey species (additive components of Equations 7 and 5, respectively), so that we can attribute changes in production to individual prey and predators. Fitting the full model with uninformative starting values required approximately 2h on a standard laptop using R version 4.3.0.

2.6 | Simulation Experiment: Estimating Productivity and Mortality

To explore the statistical performance of Ecostate, we also conduct a “self-test” simulation experiment. The experiment involves simulating ecosystem dynamics, simulating abundance indices and catch data, refitting the model to these data with or without estimating process errors, and comparing estimates with known (true) values of ecosystem variables for each of 50 simulation replicates. It explores whether a hierarchical ecosystem model (i.e., estimating process errors) improves estimates of growth rates $g(t)$ and mortality rates $m(t)$ relative to the common practice of ignoring process errors. We also estimate equilibrium biomass $\bar{\beta}_s$ and the variance of process errors for each taxon, such that the experiment confirms whether these parameters are estimable in an idealised setting.

We specifically simulate dynamics for a fictive ecosystem involving six taxa (see Table S4): one autotroph (representing pelagic primary production), one detritus (the base of the benthic foodweb), two consumers (one pelagic and one benthic), and two predators (one pelagic and one benthic) from 1980 to 2020. We also specify that benthic consumers and predators have slower life history (lower p_s and higher w_s) than their pelagic counterparts. We specify that ecotrophic efficiency $e_s = 0.9$ (i.e., 90% of biomass transfer is captured) for the producers and consumers, and that predators have equilibrium biomass $\bar{\beta}_s = 1$, and then solve for equilibrium biomass for the other species (see Figure 1). Finally, we specify a vulnerability $x_{ij} = 2$ (representing a Hollings Type-2 predator functional response) for consumers and predators, and a vulnerability $x_{ij} = 91$ (representing a close-to-constant production-per-biomass) for producers.

We then simulate an increase in fishing mortality rate for the two predators over the 40 years of simulated dynamics (see Figure S1) and specify that process errors have a standard deviation $\tau_s = 0.1$ for primary producers and predators, and $\tau_s = 0.02$ for consumers (which are also affected by process errors in both predators and producers). We simulate abundance indices and measurements of catch for each species. We then refit the model using 10 sub-intervals of the Adams-Bashforth-Moulton ODE solver. For the “full model” we estimate the difference between equilibrium and initial biomass δ_s and the magnitude of process errors τ_s for each taxon, as well as a single vulnerability $x_{\text{shared}} = x_{ij}$ for all consumers and predators (i.e., 13 fixed effects). We compare this with a “null model” that estimates only δ_s and x_{shared} (i.e., 7 fixed effects), and ignores process errors. Finally, we compare error in estimates of model parameters, as well as annual growth rate per biomass $g_s(t)$ (Equation 8), mortality rate per biomass $m_s(t)$ (Equation 6), and biomass $\beta_s(t)$ between the full and null models. We then repeat the experiment when estimating production-per-biomass p_s for all six taxa and consumption per biomass w_s for the four heterotrophs (10 extra parameters), while specifying a lognormal likelihood penalty with a log-standard deviation of 0.1. Each replicate of the simulation model required approximately 10 min on a standard laptop using R version 4.3.0.

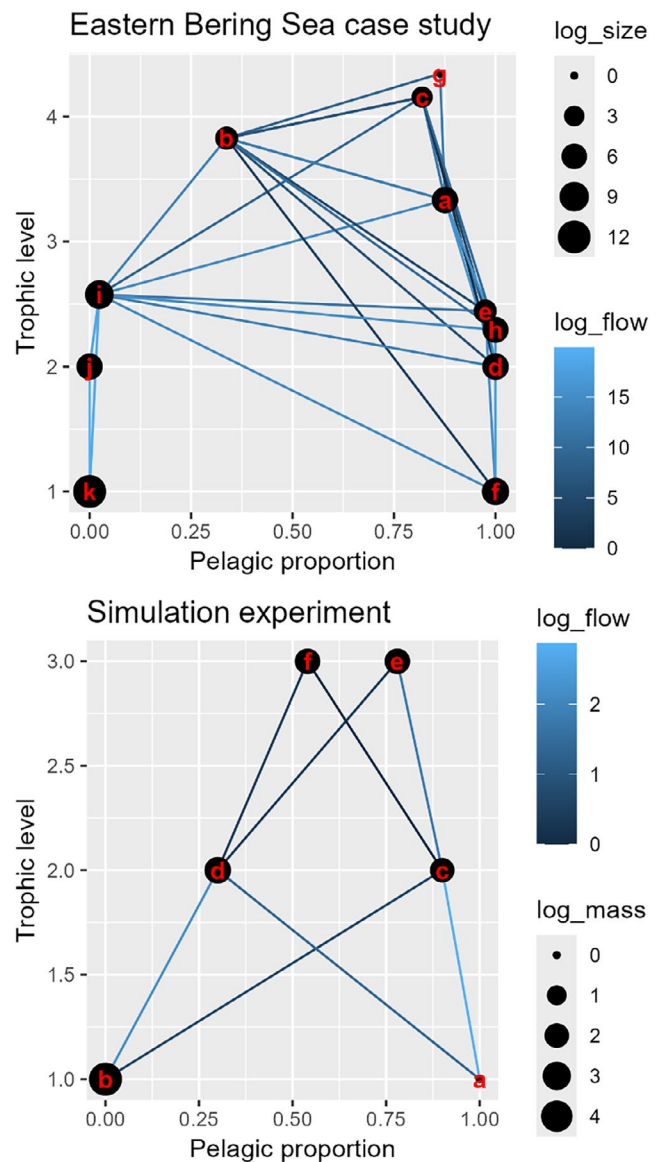


FIGURE 1 | Estimated trophic level (y-axis) and pelagic proportions (x-axis) for the eastern Bering Sea case study (top panel) or the simulation experiment (bottom panel). Taxa are labelled alphabetically following their row-order in Tables S3 and S4, respectively, with vertex circles having size representing the log-mass of each variable, and the edges colour-coded to represent the log-consumption flowing from predator to prey. We compute “Pelagic proportion” by treating “Pelagic prod.” and “Producer” as the source of pelagic production in each model, respectively.

3 | Results

For the eastern Bering Sea case study, the full version of the Ecostate model (i.e., including 11 variables and fitting to catches using process errors) includes both benthic and pelagic sources of production (Figure 1 and Table S3), and has variables that range from trophic level 1 (producer and detritus) to 4.3 (northern fur seal). Estimated trends and interannual variation are consistent with biomass surveys (except for copepods, Figure 2), and are also consistent with recent stock assessments when available (i.e., for pollock, cod, and arrowtooth flounder; Figure 3). Major

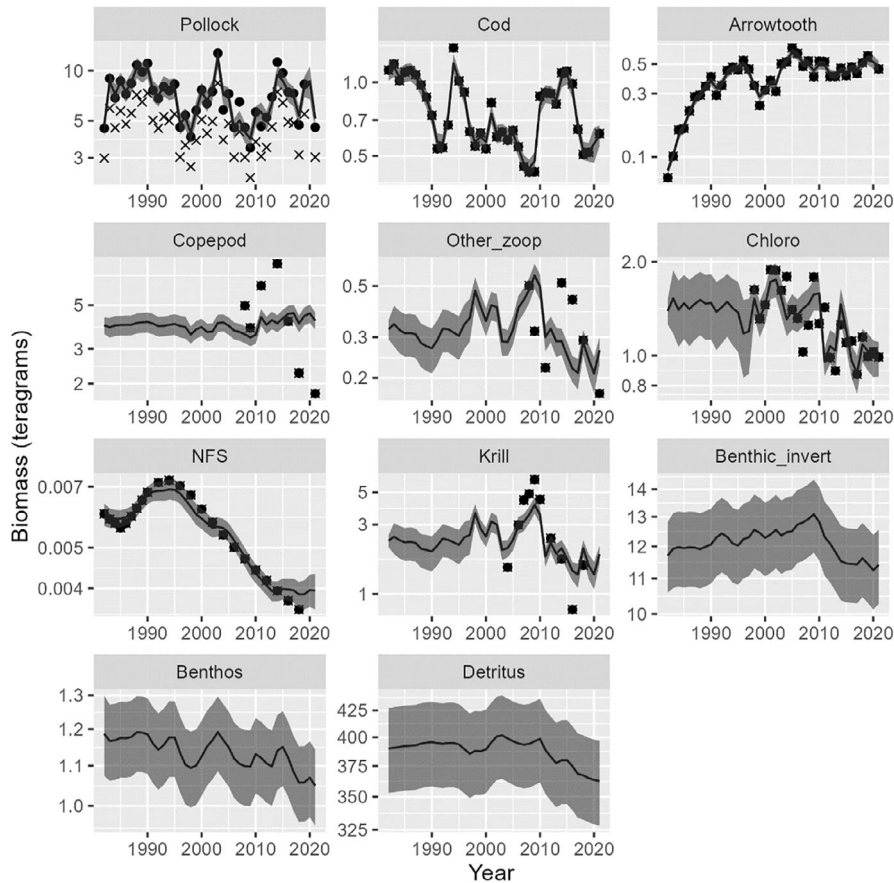


FIGURE 2 | Estimated abundance (y-axis in teragrams a.k.a. million metric tons, black line) \pm one standard error (grey shaded ribbon) in each year (x-axis) for each modelled variable (panels), plotted against the indices of biomass (black dots) for cod, arrowtooth, northern fur seals, Pollock, Copepods, Other Zooplankton, Krill, and Primary producers. For pollock, we also show the raw index of biomass (x-symbols) and the index divided by the estimated catchability coefficient (black dots), to show the estimated biomass relative to the bottom-trawl survey scale. Note that Benthic invertebrates, Benthos, and Detritus have neither absolute nor relative abundance available.

consumers (pollock and cod) show biomass cycles, i.e., elevated biomass from 2000 to 2005 and decreased biomass from 2005 to 2010, followed by elevated biomass from 2012 to 2017 and subsequently lower biomass. By contrast, arrowtooth flounder, northern fur seal, and zooplankton are dominated by decadal trends, i.e., arrowtooth showed a large increase in biomass from 1982 to 1990, northern fur seal showed a progressive decrease in biomass from 1995 onward, and both krill and primary producers both show a pronounced decline from 2008 onward. As expected, pollock biomass is higher than the bottom-trawl survey index due to an estimated catchability coefficient less than one, i.e., $\log(q_s) = -0.41$, and closely fits specified catch data (Figure S3).

The increasing biomass trend for arrowtooth and decreasing trend for northern fur seal are largely explained by the estimated difference between initial and equilibrium biomass ($\log(\delta_s) = -2.42$ and 0.27 , respectively; see Table S5). As a result, the trends for these taxa are also captured by models that ignore process errors, or the null model without process errors or catches (Figure 3). However, the model without process error (blue line in Figure 3) only captures a dampened version of the biomass cycles for Pacific cod, and fails to capture the biomass cycles for pollock or trends for the other species. Similarly, the model without process errors and catches estimates lower

biomass overall for zooplankton (krill, copepods, and other), pollock, and benthic variables. This difference in scale in the model without catches arises because we specify ecotrophic efficiency $e_s = 1$ for intermediate consumers (to avoid using auxiliary information to define their population scale). Without fishery harvest, the model can decrease copepod biomass from 4 to 2 million tons while still maintaining the biomass of species with indices of absolute abundance (cod, arrowtooth, and northern fur seals). Similarly, the model using Bayesian priors (instead of fixed values) for production and consumption per biomass (\mathbf{p} and \mathbf{w}) estimates somewhat different biomass for pollock and planktonic taxa (krills, copepods, etc) but otherwise similar patterns in biomass (Figure 3).

The state-space model attributes biomass patterns to annual variation in growth $g(t)$, natural mortality $m(t)$, fishing mortality $f(t)$ for the three exploited fishes (Figure 4), and process errors (Figure S3). The model captures substantial variation in growth rate $g(t)$ for these species because it includes the primary forage for each modelled functional group. It captures less variation mortality rates $m(t)$ because it has fewer top-predators, such that cod and arrowtooth have lower ecotrophic efficiency e_i , and therefore attributes mortality $m(t)$ primarily to the constant mortality term $u_s = p_s(1 - e_s)$ (e.g., the pink bars for cod mortality in Figure 5). Growth exceeds

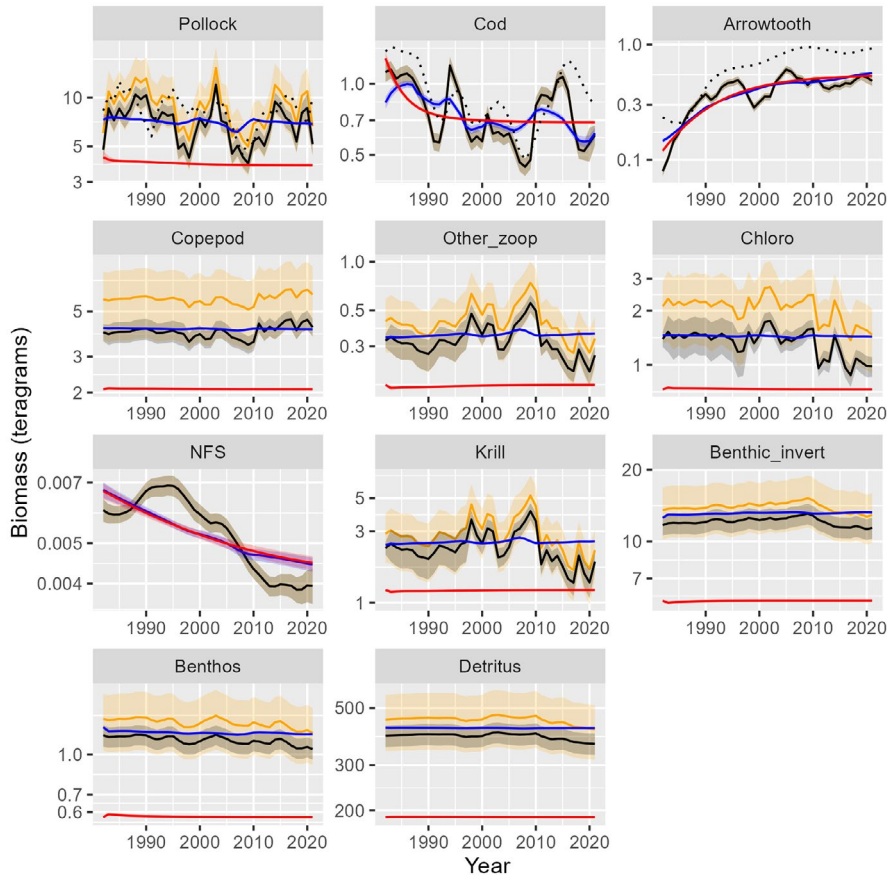


FIGURE 3 | Comparison of biomass estimates using the full model (black), a null model without process errors or catches (red), a “priors” model that estimates productivity per biomass p_s and consumption per biomass w_s for selected species using a lognormal prior (orange), and a “measurement error” model that includes catches but no process errors (blue), where each shows \pm one standard error as shading, as well as a comparable stock-assessment estimate of male and female biomass where available (black dotted lines). Note that the “full” and “priors” models are nearly identical (and therefore difficult to distinguish) for cod and arrowtooth.

natural and fishing mortality rates for arrowtooth during the initial years (1982–1995), which drives an increase in biomass, and this difference subsequently declines towards zero as population biomass stabilises. Similarly, northern fur seals have lower growth than natural mortality, in particular from 1995 to 2000 and again from 2005 to 2015, which drives a decline in biomass over time. However, biomass patterns cannot be entirely explained by changes in consumption driving growth and natural mortality. Cod and pollock have lower-than-average biomass from 2005 to 2010, and density-dependence causes estimated growth to exceed natural mortality rates (Figure 4); however, this density-dependent increase in productivity is offset by negative process errors $\epsilon_s(t)$ (Figure S3), which allows the model to estimate that lower-than-average biomass persists over these years. Similarly, decadal trends for northern fur seal are driven by a sequence of positive process errors until 2000, followed by negative process errors.

The model can be used to further decompose growth and mortality rates into the contribution of individual prey and predator species, respectively (Figure 5). This exercise shows that elevated growth rates for pollock during positive cycles (top-left panel of Figure 5) are associated with an increased proportion of krill consumption, while the contribution of copepods to pollock growth rate has been relatively consistent

over time. Predation on pollock shows a small but noticeable increase when arrowtooth biomass increased from 1982 to 1990 (bottom-left panel of Figure 5). However, fluctuations in pollock mortality are largely due to changes in cannibalism from pollock and predation from cod, during their population cycles. By contrast, growth rate for cod largely follows the cycles for pollock as their major prey (red in top-right panel of Figure 5). We do not explicitly model many predators for cod, and hence their natural mortality is largely attributed to the residual mortality that is constant over time. Finally, krill has higher growth and mortality rates than either pollock or cod due to their faster life history, and this means that small relative differences (e.g., changing growth $g_s(t)$ from 6 to 5.8) can still result in large absolute differences in population dynamics. However, the decline in chlorophyll biomass in 2010 (Figure 2) is immediately apparent in decreased consumption and growth rate for krill (Figure 5), which is synchronous with the decrease in krill biomass around that time.

Finally, our self-test simulation experiment confirms the state-space model can accurately estimate annual growth $g(t)$ and mortality $m(t)$ components (red line in Figure 6), and is generally more precise than a model that does not estimate process errors (blue line in Figure 6). This difference results from the ability of the state-space model to more accurately

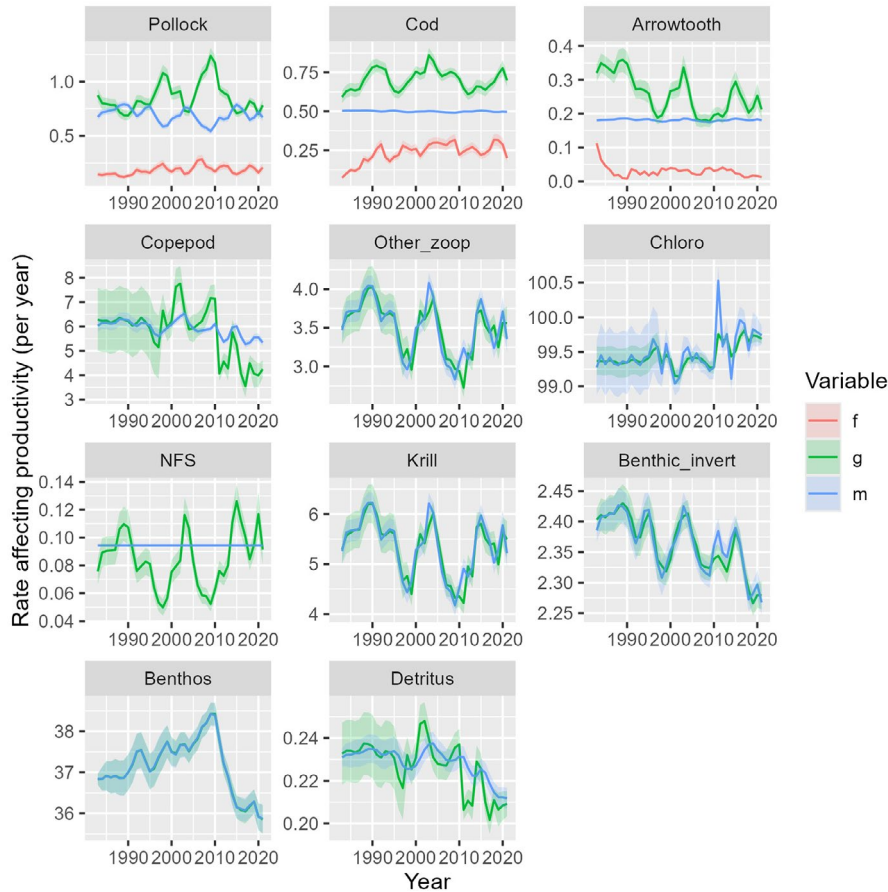


FIGURE 4 | Estimated rates that affect productivity, i.e., $g(t)$ (production rate; green) and $m(t)$ (mortality rate including consumption; blue) for each modelled species in the eastern Bering Sea using the “full” model, as well as $f(t)$ (fishing mortality rate; red) for the three species with fishery catches, showing the predicted value (line) ± 1 standard error (shaded area). Note that change in biomass $\frac{d}{dt}\beta(t) = (g(t) - f(t) - m(t) + \epsilon(t)) \times \beta(t)$ (where process error ϵ is plotted separately in Figure S2) such that g has a positive effect while m and f have negative effects.

estimate annual variation in biomass for predators and prey and therefore also improves the estimates of consumption $c_{ij}(t)$ and resulting estimates of predator growth and prey mortality rates. Both the full and null models can accurately estimate the vulnerability and equilibrium biomass parameters (see Figure S4). We also replicate the simulation experiment while estimating productivity per biomass \mathbf{p} and consumption per biomass \mathbf{w} using Bayesian priors. The full model continues to outperform the model without process errors, although both models have substantially higher errors for producers and detritus (Figure S5).

4 | Discussion

We have argued that hierarchical (a.k.a. state-space) modeling will have broad benefits across the full range of ecosystem models. These benefits include (1) better representation of system trends and cycles; (2) propagating errors through species interactions; (3) reproducibility during model fitting; and (4) attributing process errors to different mechanisms. We have then demonstrated these benefits using the first (to our knowledge) state-space extension of the most widely used mass-balance model¹ in fisheries (Coll ter et al. 2015). This extension jointly estimates mass-balance parameters and process errors via fit to time-series data. Including process errors allows us to capture

decadal trends and interannual cycles in biomass (which are otherwise mis-specified in a model that does not have process errors, Figure S3), and to more accurately capture the variable growth and mortality rates that result from changes in consumption. Estimating parameters via maximum likelihood also allows us to propagate variance in both fixed effects (e.g., equilibrium biomass) and process errors when predicting biomass in unsampled years. This predictive variance includes the contribution of both fixed effects and process errors, such that biomass has higher predictive uncertainty when distant from available data and/or for taxa with rapid life histories. We distribute our code as an R-package *ecostate*, initially available on GitHub (<https://github.com/James-Thorson-NOAA/ecostate>) with full function documentation and user vignettes (and available on CRAN) to facilitate ongoing applications and testing.

Although we extended Ecopath with Ecosim here, we suspect that a wide range of ecosystem analyses could be re-cast as hierarchical models using modern statistical-computing tools (e.g., RTMB as used here). This demonstration joins a growing list of hierarchical ecosystem models where, e.g., the length-structured model Mizer has options to estimate demographic rates (Spence, Blackwell, and Blanchard 2016) and process errors (Spence et al. 2021) via fit to time-series data. Similarly, multispecies statistical catch-at-age models often estimate recruitment deviations while accounting for predator-dependent

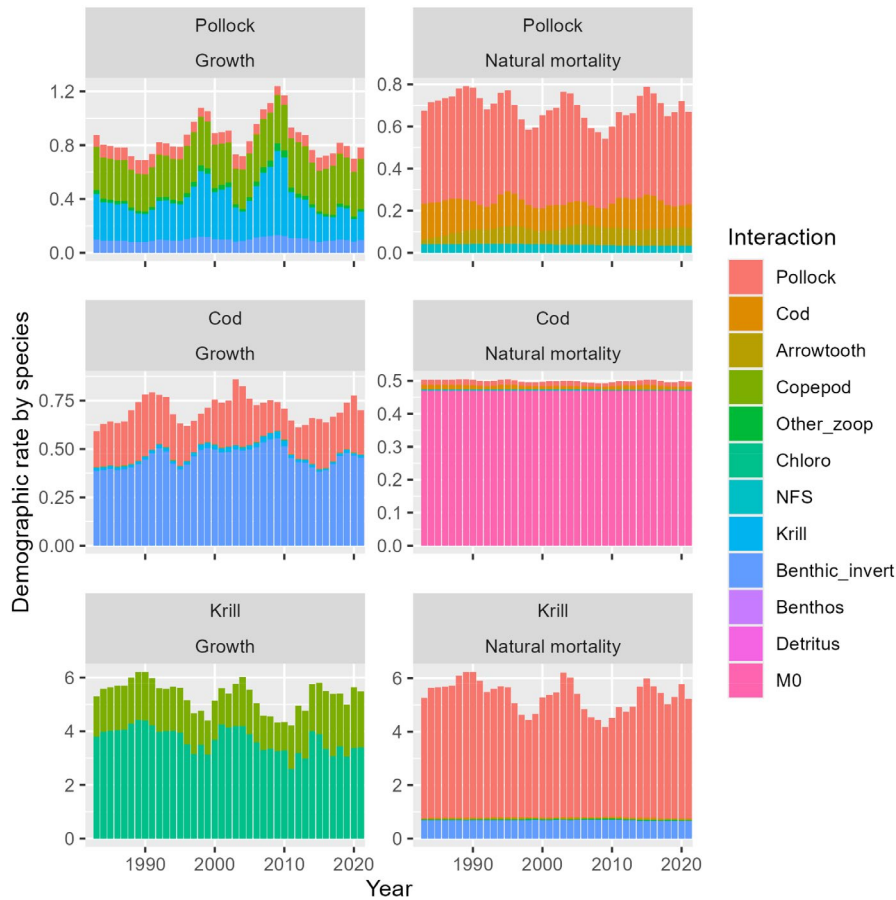


FIGURE 5 | Stacked barplot showing growth rate $g(t)$ (left column) or natural mortality rate $m(t)$ (right column) using the “full” model for pollock (top row, i.e., matching green and blue lines in first panel of Figure 3), cod (middle row, i.e., second panel of Figure 3), and krill (bottom row, i.e., 8th panel of Figure 3), while decomposing these demographic rates into the contribution for each prey species (i.e., each component of Equation 5 for Growth) or for each predator species as well as a constant residual mortality rate (i.e., each component of Equation 7 for Natural mortality), where M_0 (pink) indicates residual natural mortality.

mortality (i.e., top-down control) but not consumption-dependent growth (i.e., bottom-up control), and are sometimes called “Models of Intermediate Complexity for Ecosystems” (Plagányi et al. 2014). Despite these examples, hierarchical modelling has not previously been adopted for widely used ecosystem models including Ecopath with Ecosim, Atlantis (Fulton et al. 2011), or Osmose (Shin and Cury 1999). In these cases, modellers typically explore uncertainty by sampling parameters from a specified distribution and summarising the resulting distribution for model outputs, e.g., in Osmose (Luján et al. 2024), the Rpath implementation of Ecopath with Ecosim (Whitehouse and Aydin 2020), or Atlantis (Fulton et al. 2011). Additionally, software for these models sometimes can estimate a subset of parameters, e.g., fitting vulnerability (x_{ij}) parameters in Ecosim via fit to time-series without otherwise estimating parameters that arise in the Ecopath mass balance itself (Scott et al. 2016; Bentley et al. 2024), or the “anomaly search” function that explains model residuals using specified covariates (Shannon, Neira, and Taylor 2008). By contrast, automatic differentiation (e.g., RTMB) allows efficient calculation of the gradient of the log-likelihood function with respect to parameters, which allows us to estimate hundreds of coefficients (random and fixed effects) with little additional code beyond implementing the model dynamics themselves. We therefore encourage research exploring the use of RTMB for other classes

of ecosystem models, where penalised likelihood (i.e., fixing process-error variance a priori) would be easier (and therefore appropriate for more complex models) than the maximum-likelihood estimation used here.

We believe that hierarchical modelling will help to mitigate capacity constraints that limit the use of ecosystem and multi-species models for short-term fisheries management. Ecosystem modellers typically have just a few years to develop a “research” model and then show its usefulness for management. Optimising parameters based on statistical fit to time-series allows modellers in the related field of stock assessment to rapidly explore hundreds of different scenarios (from different combinations of estimated parameters and assumed model structure) when incorporating new data or addressing reviewer or stakeholder input. In particular, estimating process errors (e.g., recruitment deviations in age-structured assessments or process errors here) tends to allow models to have reasonable behaviour (i.e., continue to track major trends) when updated with new data, as required for an operational model that will be subsequently updated. Including fewer species (as we do here) can also address capacity limitations by (1) reducing model implementation time as an analyst could focus on developing a smaller set of data inputs, (2) simplifying the peer review process, and (3) reducing model run time thus allowing more time for running

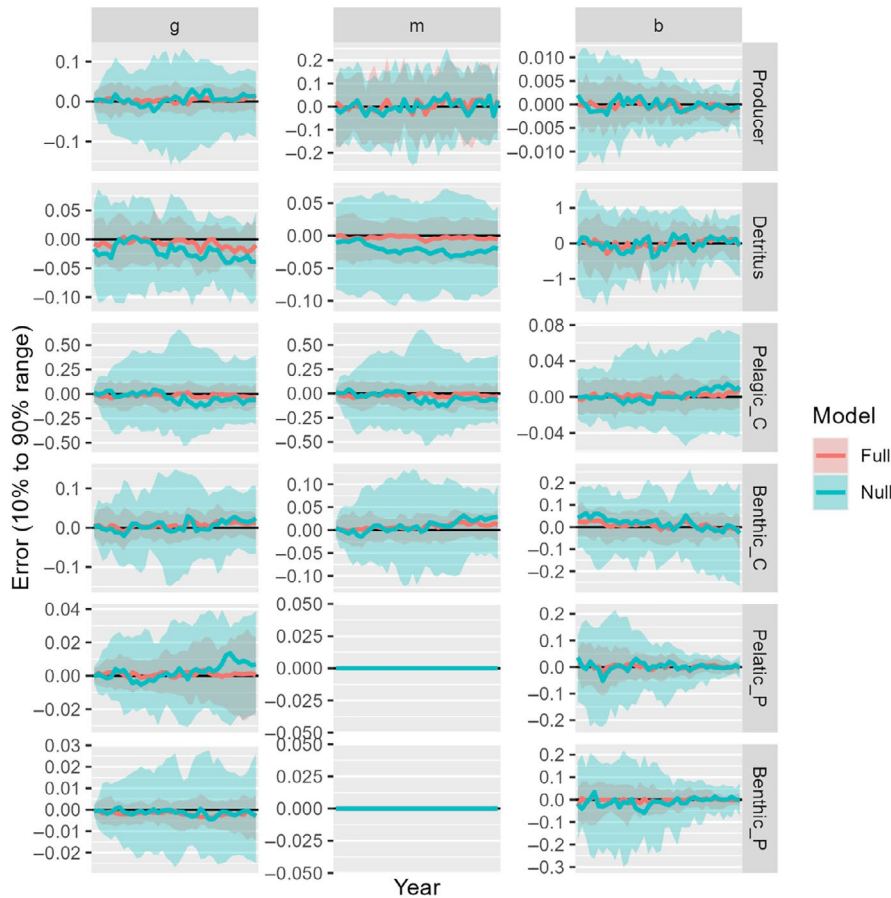


FIGURE 6 | Range of errors that covers 10% and 90% of the 50 simulation replicates (y-axis) for each year (x-axis) in annual estimates of growth from consumption (g), mortality due to predation (m) (columns), or biomass (β) for each simulated species (rows) for either the state-space model (red shading) or the same model but without estimating process errors in dynamics (blue shading), and also showing the median error for both models (red and blue lines, respectively). Note that the two predators (bottom two rows) experience no predation (see Table S3) such that their mortality is specified without error and therefore not shown.

different management scenarios. However, using a smaller set of taxa also has drawbacks, i.e., it narrows the range of alternate pathways for trophic interactions, and therefore may result in stronger predator–prey interactions than those estimated when including more taxa. Future analysis could also explore whether the variance of process errors is reduced when adding functional groups.

This state-space mass-balance model can also be interpreted as a mechanistic model to incorporate time-varying productivity into biomass-dynamic (a.k.a., surplus production) models. Biomass-dynamic models are one of the oldest models in ecology (Pearl and Reed 1920) and fisheries (Russell 1931), and state-space extensions are still widely used to identify stock status for many fisheries worldwide (Pedersen and Berg 2017; Winker et al. 2020). These models typically estimate population scale (equilibrium biomass and a catchability coefficient) by treating the fishery as a depletion experiment (Magnusson and Hilborn 2007). We encourage future research to compare Ecostate against state-space biomass-dynamics models. In particular, Ecostate would provide a parsimonious approach to predict nonstationary parameters resulting from changing predator or prey biomass (Aydin 2004), while allowing estimates of the catchability coefficient in some cases. We hypothesise that

trophic interactions could result in population cycles that are otherwise missing from single-species biomass-dynamic models (Walters and Kitchell 2001) and could also change the shape of the production function (and resulting biological reference points).

Our case study illustrates several of our claimed advantages of hierarchical ecosystem modelling. Specifically, the ecosystem includes both cyclic and long-term biomass trends that are not well captured by a mass-balance model without process errors (also noted by Aydin and Mueter 2007). In particular, primary producers have declined by nearly 30%, and this is synchronous with a declining trend in krill biomass. Previous studies have debated the relative importance of top-down and bottom-up control for krill biomass (Ressler et al. 2012; Ressler, Robertis, and Kotwicki 2014), and our study identifies declining chlorophyll-a concentrations (and its impact on growth) as a potential mechanism (see Figure 4 bottom-left panel). The model then attributes a small decline in productivity for pollock to this depressed krill biomass. These types of multi-level bottom-up impacts are not represented by statistical multispecies models, and emphasises the importance of improved monitoring for krill in understanding climate-impacts on ecosystem productivity. However, we note that bottom-up forcing is also favoured by model

assumptions, i.e., assuming ecotrophic efficiency $e_i = 1$ for prey groups (thus eliminating non-predation natural mortality) and assuming that vulnerability $x_{i,j} = 2$. In particular, future studies should seek to identify whether declining primary producers is associated with an increase in consumption w_s and/or production p_s per biomass, which could offset the foodweb impacts of declining primary producers (Nielsen et al. 2023).

Our case study also illustrates how hierarchical ecosystem modelling allows us to compare across alternative model structures using a small set of modelled taxa. Recent Rpath models for the eastern Bering Sea have included nearly 100 taxa (Aydin et al. 2007; Whitehouse et al. 2021), and the resulting model is typically used to evaluate strategic (long-term) tradeoffs amongst management strategies. By contrast, our Ecostate model includes only 10 functional groups and one detrital pool; this small size is relatively rare for mass-balance models (although see Chagaris et al. 2020), although pooling taxa still results in nearly 80% of biomass from the full Rpath model being included (see Appendix S3). Including fewer taxa allows us to calculate a high-accuracy solution to the differential equation for biomass while still integrating across random effects, as required when estimating the variance of process errors. It also allows us to provide a statistically rigorous prediction of ecosystem variables (and associated uncertainty) beyond the range of abundance indices. These predictions could then be used for seasonal-to-decadal forecasting, identifying annual status relative to ecosystem targets, or other tactical (short-term) management decisions (Plagányi 2007). Real-world application could compare model performance using an ensemble of simple-to-complex models using Ecostate, and could evaluate performance both statistically or by identifying a reduction in process-error variance (see 4th benefit of hierarchical models in the Introduction).

Finally, we recommend that hierarchical models (whether in stock assessment or ecosystem models) are used to attribute process errors to additional oceanographic, ecological, and physical drivers. We have specified that process errors are independent and identically distributed, but recent research has demonstrated how to specify a dynamic structural equation model (DSEM) representing lagged and simultaneous causal effects amongst process errors (Thorson et al. 2024). We therefore envision that future studies could treat annual covariates (e.g., ocean temperature or predator–prey overlap) as additional model variables that are treated as measured without error, and then estimate how these covariates then affect process errors. This is somewhat akin to the “forcing functions” that are estimated using covariates in Ecopath with Ecosim, although DSEM would allow missing covariate values to be imputed based on temporal and multivariate correlations, similar to recent practices in stock assessment (du Pontavice et al. 2022). For example, previous research suggests that the summer “cold pool” affects predator–prey overlap (Thorson et al. 2021), and this in turn affects predator consumption and diet composition (Goodman et al. 2022). These types of causal chains can be represented using DSEM and allow detailed specification of how covariates affect modelled processes. Once the magnitude and trend for process errors have been estimated using a hierarchical model, it then opens up a huge scope for additional research to attribute these patterns to hypothesised ecosystem drivers.

Acknowledgements

We thank Sean Lucey for previous research developing Rpath, and Arnaud Grüss, Greig Oldford, and two anonymous reviewers for helpful comments on a previous draft. Data were collected by many programs at the Alaska Fisheries Science Center, and we thank the midwater acoustics and conservation engineering (MACE) program for developing the krill index, the groundfish assessment program (GAP) for collecting the bottom-trawl survey data, the Recruitment Process Program (RPP) for collecting the copepod and other pelagic zooplankton samples, the Alaska Ecosystem Program (AEP) for collecting the northern fur seal data, and the Fisheries Monitoring and Analysis (FMA) Division for collecting fishery data that is used to estimate fishery harvest. We also thank the assessment authors for pollock (J. Ianelli), cod (S. Barbeaux), and arrowtooth (I. Spies) for prior research regarding the fished species. This publication is EcoFOCI contribution number EcoFOCI-1062. It is partially funded by the Cooperative Institute for Climate, Ocean, & Ecosystem Studies (CICOES) under NOAA Cooperative Agreement NA20OAR4320271, Contribution No. 2024-1391.

Data Availability Statement

All data and code are included in R-package *ecostate* release 0.2.0 (<https://github.com/James-Thorson-NOAA/EcoState>), which is available as a public GitHub repository during review, and also available on CRAN (<https://cran.r-project.org/web/packages/ecostate/index.html>). *EcoState* release 0.2.0 includes three vignettes that can be viewed online (<https://james-thorson-noaa.github.io/EcoState>) or replicated locally: (1) “simulation” shows how to fit the simulated 6-species ecosystem using *EcoState*, and contrasts it with package *Rpath*; (2) “surplus production” shows how to fit single-species data simulated using a Fox production function as a state-space biomass-dynamics model using *EcoState*, and contrasts fit with JABBA (Winker, Carvalho, and Kapur 2024) and SPICT (Pedersen and Berg 2017); and (3) “eastern Bering Sea” shows how to fit the eastern Bering Sea case study involving 10 functional groups and 1 detritus pool.

Endnotes

¹ Ecopath with Ecosim has 487 models compiled online via EcoBase (<https://ecobase.ecopath.org/>) as accessed June 11, 2024.

References

- Aydin, K., S. Gaichas, I. Ortiz, D. Kinzey, and N. Friday. 2007. *A Comparison of the Bering Sea, Gulf of Alaska, and Aleutian Islands Large Marine Ecosystems Through Food Web Modeling*. U.S. Dep. Commer. https://repository.library.noaa.gov/view/noaa/22894/noaa_22894_DS1.pdf.
- Aydin, K., and F. Mueter. 2007. “The Bering Sea—A Dynamic Food Web Perspective.” *Deep Sea Research Part II: Topical Studies in Oceanography* 54, no. 23: 2501–2525. <https://doi.org/10.1016/j.dsr2.2007.08.022>.
- Aydin, K. Y. 2004. “Age Structure or Functional Response? Reconciling the Energetics of Surplus Production Between Single-Species Models and Ecosim.” *African Journal of Marine Science* 26: 289–301.
- Barbeaux, S., L. Barnett, M. Hall, et al. 2023. “Assessment of the Pacific cod stock in the Eastern Bering Sea.” North Pacific Fishery Management Council.
- Begley, J., and D. Howell. 2004. “An Overview of Gadget, the Globally Applicable Area-Disaggregated General Ecosystem Toolbox.” ICES. Accessed June 11, 2024. <https://imr.brage.unit.no/imr-xmlui/bitstream/handle/11250/100625/FF1304.pdf?sequence=1>.
- Bentley, J. W., D. Chagaris, M. Coll, et al. 2024. “Calibrating Ecosystem Models to Support Ecosystem-Based Management of Marine Systems.” *ICES Journal of Marine Science* 81, no. 2: 260–275. <https://doi.org/10.1093/icesjms/fsad213>.

- Borchers, H. W. 2023. "Pracma: Practical Numerical Math Functions." R package version, (<https://CRAN.R-project.org/package=pracma>).
- Chagaris, D., K. Drew, A. Schueller, M. Cieri, J. Brito, and A. Buchheister. 2020. "Ecological Reference Points for Atlantic Menhaden Established Using an Ecosystem Model of Intermediate Complexity." *Frontiers in Marine Science* 7: 606417. <https://doi.org/10.3389/fmars.2020.606417>.
- Christensen, V., and C. J. Walters. 2004. "Ecopath With Ecosim: Methods, Capabilities and Limitations." *Ecological Modelling* 172, no. 2: 109–139. <https://doi.org/10.1016/j.ecolmodel.2003.09.003>.
- Colléter, M., A. Valls, J. Guitton, D. Gascuel, D. Pauly, and V. Christensen. 2015. "Global Overview of the Applications of the Ecopath With Ecosim Modeling Approach Using the EcoBase Models Repository." *Ecological Modelling* 302: 42–53. <https://doi.org/10.1016/j.ecolmodel.2015.01.025>.
- de Valpine, P. 2002. "Review of Methods for Fitting Time-Series Models With Process and Observation Error and Likelihood Calculations for Nonlinear, Non-Gaussian State-Space Models." *Bulletin of Marine Science* 70, no. 2: 455–471.
- du Pontavice, H., T. J. Miller, B. C. Stock, Z. Chen, and V. S. Saba. 2022. "Ocean Model-Based Covariates Improve a Marine Fish Stock Assessment When Observations Are Limited." *ICES Journal of Marine Science* 79, no. 4: 1259–1273. <https://doi.org/10.1093/icesjms/fsac050>.
- Edwards, A. M., and M. Auger-Méthé. 2019. "Some Guidance on Using Mathematical Notation in Ecology." *Methods in Ecology and Evolution* 10, no. 1: 92–99. <https://doi.org/10.1111/2041-210X.13105>.
- European Commission. 2013. *Regulation (EU) No 1380/2013 of the European Parliament and of the Council*. Brussels: European Parliament and of the Council.
- FAO. 2003. *Fisheries Management. The Ecosystem Approach to Fisheries*. Rome: UN Food and Agriculture Organization.
- Felsenstein, J. 1985. "Phylogenies and the Comparative Method." *American Naturalist* 125, no. 1: 1–15. <https://doi.org/10.1086/284325>.
- Fulton, E. A., J. S. Link, I. C. Kaplan, et al. 2011. "Lessons in Modelling and Management of Marine Ecosystems: The Atlantis Experience." *Fish and Fisheries* 12, no. 2: 171–188. <https://doi.org/10.1111/j.1467-2979.2011.00412.x>.
- Gaichas, S. K., G. Odell, K. Y. Aydin, and R. C. Francis. 2012. "Beyond the Defaults: Functional Response Parameter Space and Ecosystem-Level Fishing Thresholds in Dynamic Food Web Model Simulations." *Canadian Journal of Fisheries and Aquatic Sciences* 69, no. 12: 2077–2094. <https://doi.org/10.1139/f2012-099>.
- Goodman, M. C., G. Carroll, S. Brodie, et al. 2022. "Shifting Fish Distributions Impact Predation Intensity in a Sub-Arctic Ecosystem." *Ecography* 2022, no. 9: e06084. <https://doi.org/10.1111/ecog.06084>.
- Hollowed, A. B., N. Bax, R. Beamish, et al. 2000. "Are Multispecies Models an Improvement on Single-Species Models for Measuring Fishing Impacts on Marine Ecosystems? | ICES Journal of Marine Science | Oxford Academic." *ICES Journal of Marine Science* 3, no. 1: 707–719.
- Holt, R. D. 1997. "Community Modules." In *Multitrophic Interactions in Terrestrial Ecosystems, 36th Symposium of the British Ecological Society*, 333–349. New York: Cambridge University Press.
- Ianelli, J. N., T. Honkalehto, S. Wassermann, N. Lauffenburger, C. McGilliard, and E. Siddon. 2023. "Assessment of the Walleye Pollock Stock in the Eastern Bering Sea [NPFMC Bering Sea and Aleutian Islands SAFE]." North Pacific Fishery Management Council.
- Kass, R. E., and D. Steffey. 1989. "Approximate Bayesian Inference in Conditionally Independent Hierarchical Models (Parametric Empirical Bayes Models)." *Journal of the American Statistical Association* 84, no. 407: 717–726. <https://doi.org/10.2307/2289653>.
- Kristensen, K. 2024a. "RTMB: 'R' Bindings for 'TMB'." <https://CRAN.R-project.org/package=RTMB>.
- Kristensen, K. 2024b. "RTMBode: Solving ODEs With 'deSolve' and 'RTMB'."
- Kristensen, K., A. Nielsen, C. W. Berg, H. Skaug, and B. M. Bell. 2016. "TMB: Automatic Differentiation and Laplace Approximation." *Journal of Statistical Software* 70, no. 5: 1–21. <https://doi.org/10.18637/jss.v070.i05>.
- Lauth, R. R., and J. Conner. 2016. *Results of the 2013 Eastern Bering Sea Continental Shelf Bottom Trawl Survey of Groundfish and Invertebrate Resources*. Seattle, WA: NOAA Technical Memorandum, Alaska Fisheries Science Center.
- Lucey, S. M., S. K. Gaichas, and K. Y. Aydin. 2020. "Conducting Reproducible Ecosystem Modeling Using the Open Source Mass Balance Model Rpath." *Ecological Modelling* 427: 109057. <https://doi.org/10.1016/j.ecolmodel.2020.109057>.
- Luján, C., R. Oliveros-Ramos, N. Barrier, P. Leadley, and Y.-J. Shin. 2024. "Key Species and Indicators Revealed by an Uncertainty Analysis of the Marine Ecosystem Model OSMOSE." *Marine Ecology Progress Series* SPF2: 29–46. <https://doi.org/10.3354/meps14465>.
- Magnusson, A., and R. Hilborn. 2007. "What Makes Fisheries Data Informative?" *Fish and Fisheries* 8, no. 4: 337–358.
- McHuron, E. A., K. Luxa, N. A. Pelland, et al. 2020. "Practical Application of a Bioenergetic Model to Inform Management of a Declining fur Seal Population and Their Commercially Important Prey." *Frontiers in Marine Science* 7: 597973. <https://doi.org/10.3389/fmars.2020.597973>.
- Monnahan, C. C. 2024. "Toward Good Practices for Bayesian Data-Rich Fisheries Stock Assessments Using a Modern Statistical Workflow." *Fisheries Research* 275: 107024. <https://doi.org/10.1016/j.fishres.2024.107024>.
- Monnahan, C. C., J. T. Thorson, S. Kotwicki, N. Lauffenburger, J. N. Ianelli, and A. E. Punt. 2021. "Incorporating Vertical Distribution in Index Standardization Accounts for Spatiotemporal Availability to Acoustic and Bottom Trawl Gear for Semi-Pelagic Species." *ICES Journal of Marine Science* 78: 1826–1839. <https://doi.org/10.1093/icesjms/fsab085>.
- Nielsen, A., and C. W. Berg. 2014. "Estimation of Time-Varying Selectivity in Stock Assessments Using State-Space Models." *Fisheries Research* 158: 96–101.
- Nielsen, J. M., N. A. Pelland, S. W. Bell, et al. 2023. "Seasonal Dynamics of Primary Production in the Southeastern Bering Sea Assessed Using Continuous Temporal and Vertical Dissolved Oxygen and Chlorophyll-a Measurements." *Journal of Geophysical Research, Oceans* 128, no. 5: e2022JC019076. <https://doi.org/10.1029/2022JC019076>.
- NOAA. 2016. *Ecosystem Based Fisheries Management Policy of the National Marine Fisheries Service, Policy 01-120*. Silver Spring, MD: National Oceanic and Atmospheric Administration.
- Pauly, D., V. Christensen, and C. Walters. 2000. "Ecopath, Ecosim, and Ecospace as Tools for Evaluating Ecosystem Impact of Fisheries." *ICES Journal of Marine Science* 57, no. 3: 697–706.
- Pearl, R., and L. J. Reed. 1920. "On the Rate of Growth of the Population of the United States Since 1790 and Its Mathematical Representation." *Proceedings of the National Academy of Sciences of the United States of America* 6, no. 6: 275–288.
- Pedersen, M. W., and C. W. Berg. 2017. "A Stochastic Surplus Production Model in Continuous Time." *Fish and Fisheries* 18, no. 2: 226–243. <https://doi.org/10.1111/faf.12174>.
- Plagányi, É. E. 2007. *Models for an Ecosystem Approach to Fisheries*. Rome: Food & Agriculture Organization. Accessed July 1, 2012. <http://books.google.com/books?hl=en&lr=&id=MJI3aZApEQkC&oi=fnd&pg=PP9&dq=models+for+an+ecosystem+approach+to+fisheries&ots=HggvLmdgLv&sig=vCbRBUVqZIUcKnWkv8I2OVbbmRY>.
- Plagányi, É. E., and D. S. Butterworth. 2004. "A Critical Look at the Potential of Ecopath With Ecosim to Assist in Practical Fisheries Management." *African Journal of Marine Science* 26: 261–287.

- Plagányi, É. E., A. E. Punt, R. Hillary, et al. 2014. "Multispecies Fisheries Management and Conservation: Tactical Applications Using Models of Intermediate Complexity." *Fish and Fisheries* 15, no. 1: 1–22. <https://doi.org/10.1111/j.1467-2979.2012.00488.x>.
- Polovina, J. J. 1984. "Model of a Coral Reef Ecosystem." *Coral Reefs* 3, no. 1: 1–11. <https://doi.org/10.1007/BF00306135>.
- Punt, A. E., A. Dunn, B. P. Elvarsson, et al. 2020. "Essential Features of the Next-Generation Integrated Fisheries Stock Assessment Package: A Perspective." *Fisheries Research* 229: 105617. <https://doi.org/10.1016/j.fishres.2020.105617>.
- R Core Team. 2023. *R: A Language and Environment for Statistical Computing*. Vienna, Austria: R Foundation for Statistical Computing. <https://www.R-project.org/>.
- Ressler, P. H., A. De Robertis, J. D. Warren, J. N. Smith, and S. Kotwicki. 2012. "Developing an Acoustic Survey of Euphausiids to Understand Trophic Interactions in the Bering Sea Ecosystem." *Deep Sea Research Part II: Topical Studies in Oceanography* 65–70: 184–195. <https://doi.org/10.1016/j.dsr2.2012.02.015>.
- Ressler, P. H., A. D. Robertis, and S. Kotwicki. 2014. "The Spatial Distribution of Euphausiids and Walleye Pollock in the Eastern Bering Sea Does Not Imply Top-Down Control by Predation." *Marine Ecology Progress Series* 503: 111–122. <https://doi.org/10.3354/meps10736>.
- Russell, E. S. 1931. "Some Theoretical Considerations on the 'Overfishing' Problem." *ICES Journal of Marine Science* 6, no. 1: 3–20. <https://doi.org/10.1093/icesjms/6.1.3>.
- Scott, E., N. Serpetti, J. Steenbeek, and J. J. Heymans. 2016. "A Stepwise Fitting Procedure for Automated Fitting of Ecopath With Ecosim Models." *SoftwareX* 5: 25–30. <https://doi.org/10.1016/j.softx.2016.02.002>.
- Scott, F., J. L. Blanchard, and K. H. Andersen. 2014. "Mizer: An R Package for Multispecies, Trait-Based and Community Size Spectrum Ecological Modelling." *Methods in Ecology and Evolution* 5, no. 10: 1121–1125. <https://doi.org/10.1111/2041-210X.12256>.
- Shannon, L. J., S. Neira, and M. Taylor. 2008. "Comparing Internal and External Drivers in the Southern Benguela and the Southern and Northern Humboldt Upwelling Ecosystems." *African Journal of Marine Science* 30, no. 1: 63–84. <https://doi.org/10.2989/AJMS.2008.30.1.7.457>.
- Shin, Y.-J., and P. Cury. 1999. "OSMOSE: A Multispecies Individual-Based Model to Explore the Functional Role of Biodiversity in Marine Ecosystems." *Ecosystem Approaches for Fisheries Management, University of Alaska Sea Grant, Fairbanks*: 593–607.
- Shotwell, S. K., M. Bryan, D. H. Hanselman, et al. 2023. "Assessment of the Arrowtooth Flounder Stock in the Bering Sea and Aleutian Islands." North Pacific Fishery Management Council. https://apps-afsc.fisheries.noaa.gov/Plan_Team/2023/BSAItf.pdf.
- Skaug, H., and D. Fournier. 2006. "Automatic Approximation of the Marginal Likelihood in Non-Gaussian Hierarchical Models." *Computational Statistics and Data Analysis* 51, no. 2: 699–709.
- Soetaert, K., T. Petzoldt, and R. W. Setzer. 2010. "Solving Differential Equations in R: Package deSolve." *Journal of Statistical Software* 33, no. 9: 1–25. <https://doi.org/10.18637/jss.v033.i09>.
- Spence, M. A., P. G. Blackwell, and J. L. Blanchard. 2016. "Parameter Uncertainty of a Dynamic Multispecies Size Spectrum Model." *Canadian Journal of Fisheries and Aquatic Sciences* 73, no. 4: 589–597. <https://doi.org/10.1139/cjfas-2015-0022>.
- Spence, M. A., R. B. Thorpe, P. G. Blackwell, F. Scott, R. Southwell, and J. L. Blanchard. 2021. "Quantifying Uncertainty and Dynamical Changes in Multi-Species Fishing Mortality Rates, Catches and Biomass by Combining State-Space and Size-Based Multi-Species Models." *Fish and Fisheries* 22, no. 4: 667–681. <https://doi.org/10.1111/faf.12543>.
- Stock, B. C., and T. J. Miller. 2021. "The Woods Hole Assessment Model (WHAM): A General State-Space Assessment Framework That Incorporates Time-and Age-Varying Processes via Random Effects and Links to Environmental Covariates." *Fisheries Research* 240: 105967.
- Stock, B. C., H. Xu, T. J. Miller, J. T. Thorson, and J. A. Nye. 2021. "Implementing Two-Dimensional Autocorrelation in Either Survival or Natural Mortality Improves a State-Space Assessment Model for Southern New England-Mid Atlantic Yellowtail Flounder." *Fisheries Research* 237: 105873. <https://doi.org/10.1016/j.fishres.2021.105873>.
- Thorson, J. T., A. G. Andrews III, T. E. Essington, and S. I. Large. 2024. "Dynamic Structural Equation Models Synthesize Ecosystem Dynamics Constrained by Ecological Mechanisms." *Methods in Ecology and Evolution* 15, no. 4: 744–755. <https://doi.org/10.1111/2041-210X.14289>.
- Thorson, J. T., M. L. Arimitsu, L. A. K. Barnett, et al. 2021. "Forecasting Community Reassembly Using Climate-Linked Spatio-Temporal Ecosystem Models." *Ecography* 44, no. 4: 612–625. <https://doi.org/10.1111/ecog.05471>.
- Thorson, J. T., and C. Minto. 2015. "Mixed Effects: A Unifying Framework for Statistical Modelling in Fisheries Biology." *ICES Journal of Marine Science* 72, no. 5: 1245–1256. <https://doi.org/10.1093/icesjms/fsu213>.
- Thorson, J. T., K. Ono, and S. B. Munch. 2014. "A Bayesian Approach to Identifying and Compensating for Model Misspecification in Population Models." *Ecology* 95, no. 2: 329–341. <https://doi.org/10.1890/13-0187.1>.
- Walters, C., V. Christensen, and D. Pauly. 1997. "Structuring Dynamic Models of Exploited Ecosystems From Trophic Mass-Balance Assessments." *Reviews in Fish Biology and Fisheries* 7, no. 2: 139–172. <https://doi.org/10.1023/A:1018479526149>.
- Walters, C., and J. F. Kitchell. 2001. "Cultivation/Depensation Effects on Juvenile Survival and Recruitment: Implications for the Theory of Fishing." *Canadian Journal of Fisheries and Aquatic Sciences* 58, no. 1: 39–50.
- Whitehouse, G. A., and K. Y. Aydin. 2020. "Assessing the Sensitivity of Three Alaska Marine Food Webs to Perturbations: An Example of Ecosim Simulations Using Rpath." *Ecological Modelling* 429: 109074.
- Whitehouse, G. A., K. Y. Aydin, A. B. Hollowed, et al. 2021. "Bottom-Up Impacts of Forecasted Climate Change on the Eastern Bering Sea Food Web." *Frontiers in Marine* 8: 624301. <https://doi.org/10.3389/fmars.2021.624301>.
- Winker, H., F. Carvalho, and M. Kapur. 2024. "JABBA: Just Another Bayesian Biomass Assessment." <https://github.com/jabbamodel/JABBA>.
- Winker, H., F. Carvalho, J. T. Thorson, et al. 2020. "JABBA-Select: Incorporating Life History and Fisheries' Selectivity Into Surplus Production Models." *Fisheries Research* 222: 105355. <https://doi.org/10.1016/j.fishres.2019.105355>.
- Xu, H., J. T. Thorson, and R. D. Methot. 2020. "Comparing the Performance of Three Data-Weighting Methods When Allowing for Time-Varying Selectivity." *Canadian Journal of Fisheries and Aquatic Sciences* 77, no. 2: 247–263. <https://doi.org/10.1139/cjfas-2019-0107>.

Supporting Information

Additional supporting information can be found online in the Supporting Information section.